International Conference on Space Optics—ICSO 2014

La Caleta, Tenerife, Canary Islands

7–10 October 2014

Edited by Zoran Sodnik, Bruno Cugny, and Nikos Karafolas

Optical performance of the SO/PHI full disk telescope due to temperature gradients effect on the heat rejection entrance window

D. Garranzo

A. Núñez

P. Zuluaga-Ramírez

J. Barandiarán

et al.

International Conference on Space Optics — ICSO 2014, edited by Zoran Sodnik, Nikos Karafolas, Bruno Cugny, Proc. of SPIE Vol. 10563, 105634T · © 2014 ESA and CNES
CCC code: 0277-786X/17/$18 · doi: 10.1117/12.2304067

OPTICAL PERFORMANCE OF THE SO/PHI FULL DISK TELESCOPE DUE TO TEMPERATURE GRADIENTS EFFECT ON THE HEAT REJECTION ENTRANCE WINDOW

D. Garranzo[1], A. Núñez[1], P. Zuluaga-Ramírez[1], J. Barandiarán[1], A. Fernández-Medina[1], T. Belenguer[1], A. Álvarez-Herrero[1]

[1]*Instituto Nacional de Técnica Aeroespacial, Área de Instrumentación Óptica Espacial, Madrid, Spain.*

ABSTRACT

The Polarimetric Helioseismic Imager for Solar Orbiter (SO/PHI) is an instrument on board in the Solar Orbiter mission. The Full Disk Telescope (FDT) will have the capability of providing images of the solar disk in all orbital faces with an image quality diffraction-limited. The Heat Rejection Entrance Window (HREW) is the first optical element of the instrument. Its function is to protect the instrument by filtering most of the Solar Spectrum radiation. The HREW consists of two parallel-plane plates made from Suprasil and each surface has a coating with a different function: an UV shield coating, a low pass band filter coating, a high pass band filter coating and an IR shield coating, respectively.

The temperature gradient on the HREW during the mission produces a distortion of the transmitted wave-front due to the dependence of the refractive index with the temperature (thermo-optic effect) mainly. The purpose of this work is to determine the capability of the PHI/FDT refocusing system to compensate this distortion.

A thermal gradient profile has been considered for each surface of the plates and a thermal-elastic analysis has been done by Finite Element Analysis to determine the deformation of the optical elements. The Optical Path Difference (OPD) between the incident and transmitted wavefronts has been calculated as a function of the ray tracing and the thermo-optic effect on the optical properties of Suprasil (at the work wavelength of PHI) by means of mathematical algorithms based on the 3D Snell Law. The resultant wavefronts have been introduced in the optical design of the FDT to evaluate the performance degradation of the image at the scientific focal plane and to estimate the capability of the PHI refocusing system for maintaining the image quality diffraction-limited.

The analysis has been carried out considering two different situations: thermal gradients due to on axis attitude of the instrument and thermal gradients due to 1º off pointing attitude. The effect over the boresight at the instrument focal plane has also been analyzed.

The results show that the effect of the FDT HREW thermal gradients on the FDT performance can be optically corrected. The influence of the thermal gradients on the system is also presented.

I. INTRODUCTION

PHI (Polarimetric Helioseismic Imager) is designed to carry out solar photospheric intensity, velocity and magnetic field measurements [1]. The measurement principle of PHI is based on imaging spectropolarimetric observations of a photospheric absorption line in the solar visible-light spectrum. Therefore PHI is a diffraction limited, wavelength tunable, quasi-monochromatic and polarisation sensitive imager.

The PHI instrument consists of two telescopes, a High Resolution Telescope (HRT) that will image a fraction of the solar disk at a resolution reaching ~150 km at perihelion, and a Full Disk Telescope (FDT) to image the full solar disk during all phases of the orbit (distances from 1 to 0.28 AU). The two telescopes can work sequentially and their selection is made by the Feed Selection Mechanism (FSM), which feeds one filtergraph (FG), the camera optics and one focal plane array (FPA). The FG provides for a very narrow passband filter centered at a wavelength of λ=617 nm. The polarimetric analysis is performed by one polarization modulation package (PMP) [2] in each of the telescopes. The modulation scheme is the same as the one used in the IMaX instrument of the Sunrise mission [3]. In addition to these two main units, the SO/PHI design also includes two Heat Rejection Entrance Windows (HREW) one for each telescope. These entrance windows are separate items which will be mounted on the SO heat shield. Fig. 1 shows a basic functional diagram of PHI.

The function of the HREW is to limit the amount of light entering to the instrument and is mounted at a specific position in the feedthrough, a tube that pass through the heat shield of the SO spacecraft and which function if to guide sun radiation into the PHI instrument.

The FDT has its own Re-focusing Mechanism (FRM) based on axial movements of a lens to compensate the thermal/vacuum environment defocusing produced during the mission.

In this paper an analysis of the effects of a temperature in-homogeneity within the HREW substrates on the transmitted wavefront and the ability of the PHI/FDT refocusing system to recover the image quality is presented.

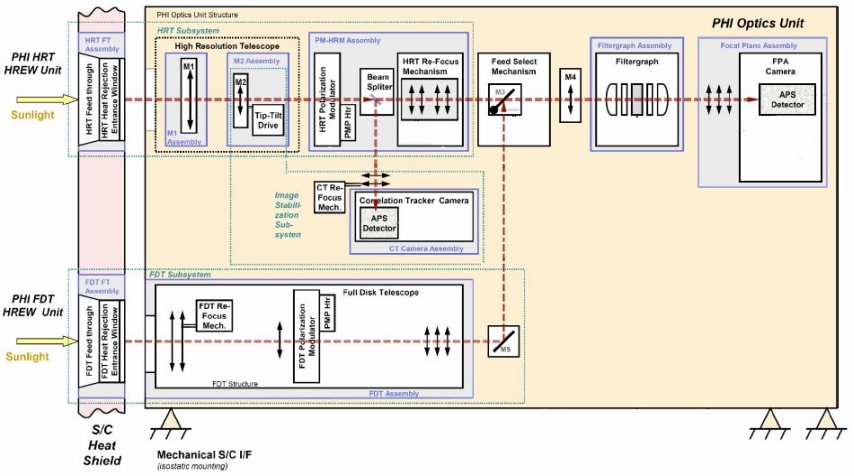

Fig. 1. Basic Functional diagram of PHI

II. HREW DESIGN CONCEPT

The HREW has been designed by SELEX in the framework of an ESA led technology development activity under original ESTEC contract No. 20018/06/NL/CP, and extensions thereof.

The HREW consists of two parallel-plane substrate plates (window 1 & window 2) made of Suprasil 300 with a central thickness of 9 mm. These two substrates are each coated on both sides with different coatings: an UV reflector, a short pass, a long pass, and an IR shield. These coatings and the choice of Suprasil help to minimize the optical absorptivity in the substrate and to radiatively decouple the HREW, which is expected to run at high temperatures during perihelion passages, from the PHI instrument cavity.

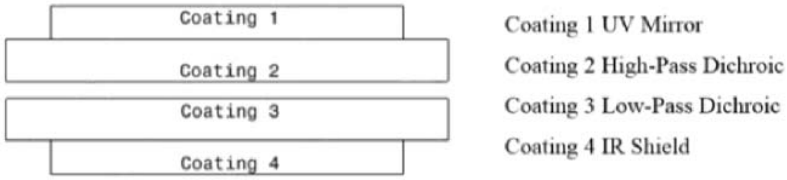

Fig. 2. HREW Coatings

The two Suprasil plates are mounted into a titanium holder consisting of two parts; the upper part (Sun-side) is connected to the feed-through with three attachment interfaces. The lower part (instrument side) is also made of titanium and confines the two glasses in axial direction. Direct contact between the titanium and the glass is avoided by the use of (lateral) VESPEL spacers and O-rings of stainless steel (axial direction) [4].

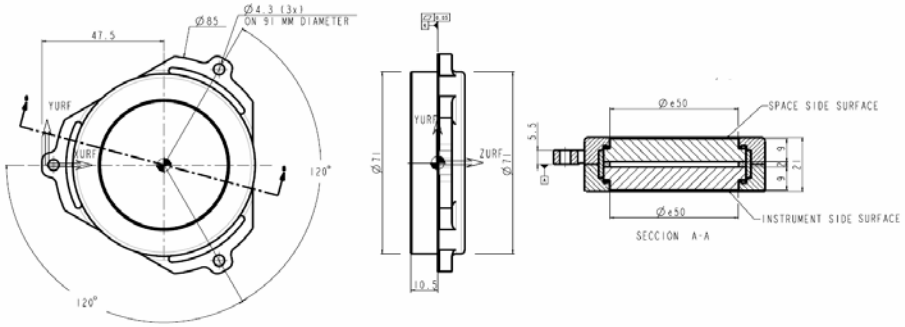

Fig. 3. HREW Design

The temperature distribution of the HREW is driven by two main factors: the flux of heat transmission through the mechanical mount from the substrates to the feedthrough, and the radiative environment within the heat-shield/feedthrough assembly. While the space side coating radiates efficiently to cold sky with high surface emissivity and a large view factor, the instrument side coating has a low emissivity in order to minimize the infrared load to the instrument.

III. FRM DESIGN CONCEPT

The FDT Re-focussing Mechanism (FRM) is designed to adjust the optics of the FDT to obtain focused images at the scientific focal plane. This, as any mechanism, will suffer from position uncertainties due to wearing and backlash, and its precision will affect the performance of the refocusing process. This is an optomechanical assembly designed to hold two lenses, plus the entrance diaphragm of the FDT system. One of these lenses (L2) mounts on a motorized platform, which locates it at the exact point to perform the correct focusing of the system at any situation. This position is achieved by evaluating the loss of contrast in a monochrome image through an algorithm based in the image gradient [5]. Focus is then achieved by moving L2 with high accuracy and repeatability over a ~4 mm travel range, and in the applicable range of temperatures. An L2 shift of 80 μm can compensate for 1 mm of focus displacement at the FPA. Therefore, the system is able to compensate for strong defocused situations.

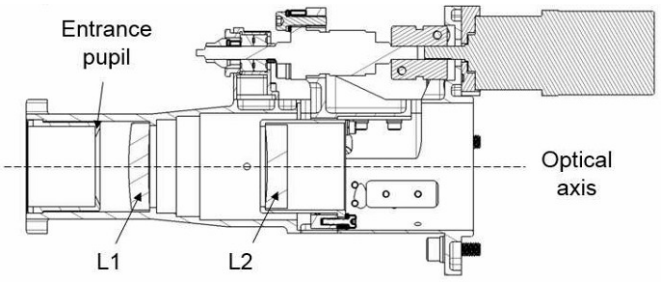

Fig. 4. FRM Design

IV. MODEL PHILOSOPY

Refractive optical components act on the transmitted wave front inducing optical path differences (OPDs). The OPDs depend on changes in the thickness and the refraction index of the material that light goes through on its way. And on the other hand, the thickness and the refraction index change with the temperature.

To determinate the capability of the PHI/FDT refocusing system to compensate radial/azimuthal thermal gradient of the FDT HREW the following simulation was performed:

1. Firstly the temperature profile, the changes in the thickness and the refractive index by effect of the temperature profile for each window are simulated. In this way it can be obtained the optical path differences (OPDs) corresponding to each window due to its temperature profile.
2. The OPDs are represented by Fringe Zernike polynomials which are the representation of the transmitted wavefront of each window by effect of the temperature.
3. The Fringe Zernikes polynomials are applied to each window as a wavefront interferograms in CODEV. That way it is possible to simulate the total deformation of the wavefront through the FDT-HREW by effect of the temperature.
4. The perturbed FDT-HREW and the complete FDT "hot case" (more restrictive case) are put together to evaluate the performance degradation at the scientific plane.
5. An optimization of the whole system is carried out using the PHI/FDT refocusing system (axial movement of L2 lens) in order to estimate its capacity to maintain the image quality diffraction-limited.

A. THERMO-MECHANICAL MODEL

As we mentioned above, the temperature distribution of the HREW is driven by two main factors: the flux of heat transmission through the mechanical mount from the substrates to the feedthrough, and the radiative environment within the heat-shield/feedthrough assembly. The overall shape of the temperature distribution within the HREW shall be as close to a rotationally symmetrical as possible (eg parabola) and show a radial/azimutal gradient. The temperature profiles can be imported from a thermal model or directly defined by the equation (1):

$$T = T_C + \left(T_R + T_A \sin(\alpha)\right)\left(R/R_0\right)^{POW} \tag{1}$$

Where T_C is the central temperature, T_R maximum amplitude of the radial gradient, T_A maximum amplitude of the azimutal gradient, R_0 is the clear aperture raadius, R the radial coordinate, θ the angular coordinate, n_S the number of azimuthal sectors and α is the angular coordinate for each azimuthal sector (eg. $\alpha = \text{rem}(\theta, 2\pi/n_S)\cdot n_S$). With the parameters n_S and α we can introduce zones affected by 'shadows'.

The windows are considered mounted in perfectly isostatic supports, so the windows can expand contract 'freely' with the temperature. Given the temperatures at both surfaces of the window, the temperature gradients in the internal volume, and the deformations of the window were determined by thermal-elastic finite element model [6, 7].

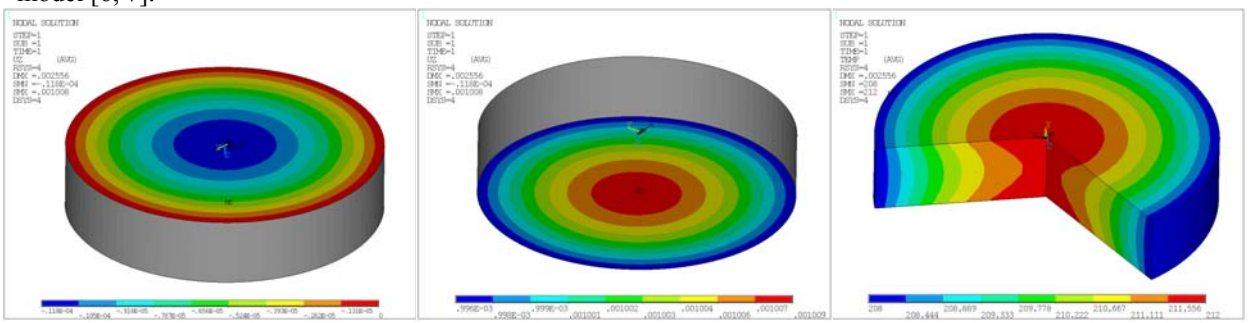

Fig. 5. Window deformation and internal temperature by thermal-elastic finite model

B. OPDs MODEL

Each window is split in seven layers. The temperatures for each layer and the deformation for the first and last layer, obtained from the finite element model, are fit to a grid map of 128x128 points.

Normal incidence and a wavelength of λ=617.3 nm will be considered for the calculus.

The refraction index for each layer at i-point can be calculated as:

$$n_i = n_0 + (T_i - T_{ref})\cdot dn/dT \tag{2}$$

Where T_{ref} is 20ºC and n_0 depends on the wavelength and it is obtained from the Selmeiller Equation with λ in microns.

$$n_0^2 - 1 = \frac{B_1\cdot\lambda^2}{\lambda^2 - C_1} + \frac{B_2\cdot\lambda^2}{\lambda^2 - C_2} + \frac{B_3\cdot\lambda^2}{\lambda^2 - C_3} \tag{3}$$

With the coefficients for Suprasil 300:

$B_1 = 4.73115591\cdot10^{-1}$; $C_1 = 1.29957170\cdot10^{-2}$
$B_2 = 6.31038719\cdot10^{-1}$ $C_2 = 4.12809220\cdot10^{-3}$
$B_3 = 9.06404498\cdot10^{-1}$ $C_3 = 9.87685322\cdot10^{1}$

dn/dt also depends on the wavelength [8], $dn/dt\ (\lambda = 617.3\ nm) = 10.036\cdot(10^{-6}/K)$

Finally, the index of refraction for each slit is considered as the mean value between two layers:

$$n_{slit}(k) = \frac{n_{layer(k-1)} + n_{layer(k)}}{2} \tag{4}$$

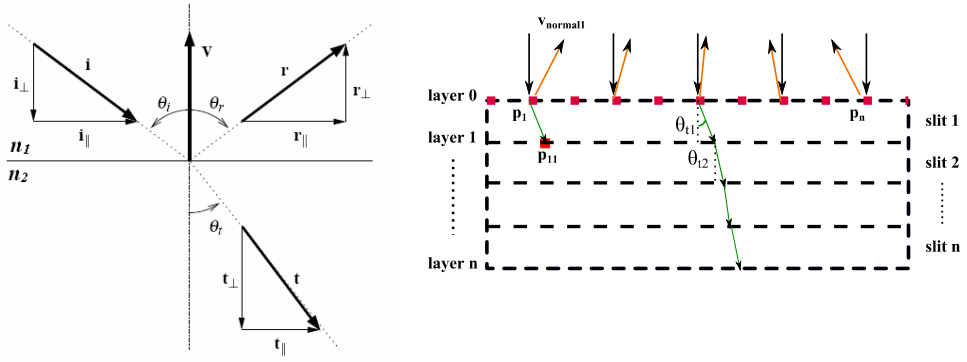

Fig. 6. Ray tracing throughout layers

For each incident ray (grid 128x128) we calculate the ray refracted by the equation (5) obtained from Snell's law and using vector arithmetic only [9, 10]:

$$\bar{t} = \frac{n_1}{n_2}\bar{i} + \left(\frac{n_1}{n_2}\cos\theta_i - \sqrt{1-\sin^2\theta_t}\right)\bar{v}$$
$$with \qquad \cos\theta_i = -\bar{i}\cdot\bar{v} \tag{5}$$
$$\sin^2\theta_t = \left(\frac{n_1}{n_2}\right)^2\left(1-\cos^2\theta_i\right)$$

The direction vector of the incident ray (= incoming ray) is ***i*** and ***v*** is the normal vector, orthogonal to the interface and pointing towards the first material. These vectors are (or will be) normalized as well.

For each point of a layer ($p_{i,j}$) compute the corresponding refracted ray and calculate the point of intersection with the next layer ($p_{i,j+1}$). From the finite element model we obtain the temperature and refractive index ($n_{i,j}$ & $n_{i,j+1}$) of each point. And if that point is into the clear aperture of the HREW we calculate his corresponding optical path.

$$OP_{i,j} = \left|\overline{p_{i,j}p_{i,j+1}}\right|\frac{n_{i,j}+n_{i,j+1}}{2} \tag{6}$$

Finally for each incident ray, the total optical path will be the sum of each of the paths through the layers, obtaining at the end a map of optical paths for the entire window (*OP1*)

$$OP1_i = \sum_j OP_{i,j} \qquad i = 1:128x128-1\,(grid) \quad j = 1:7\,(layers) \tag{7}$$

In order to work with CODEV the optical path difference (*OPD*) will be introduced as the difference between *OP2* and OP1, being OP2 the optical path difference corresponding of a window with a constant temperature (central temperature, T_C) and no deformation (L_0 = 9.00 mm).

$$\begin{aligned} OPD &= OP2 - OP1 \\ OP2 &= n(T_C)\cdot L_0 \end{aligned} \tag{8}$$

The OPDs will be fit to a Zernike surfaces. Two files with 36 Fringe Zernike polynomials each one will be obtained. They represent the transmitted wavefront of the windows by effect of the temperature.

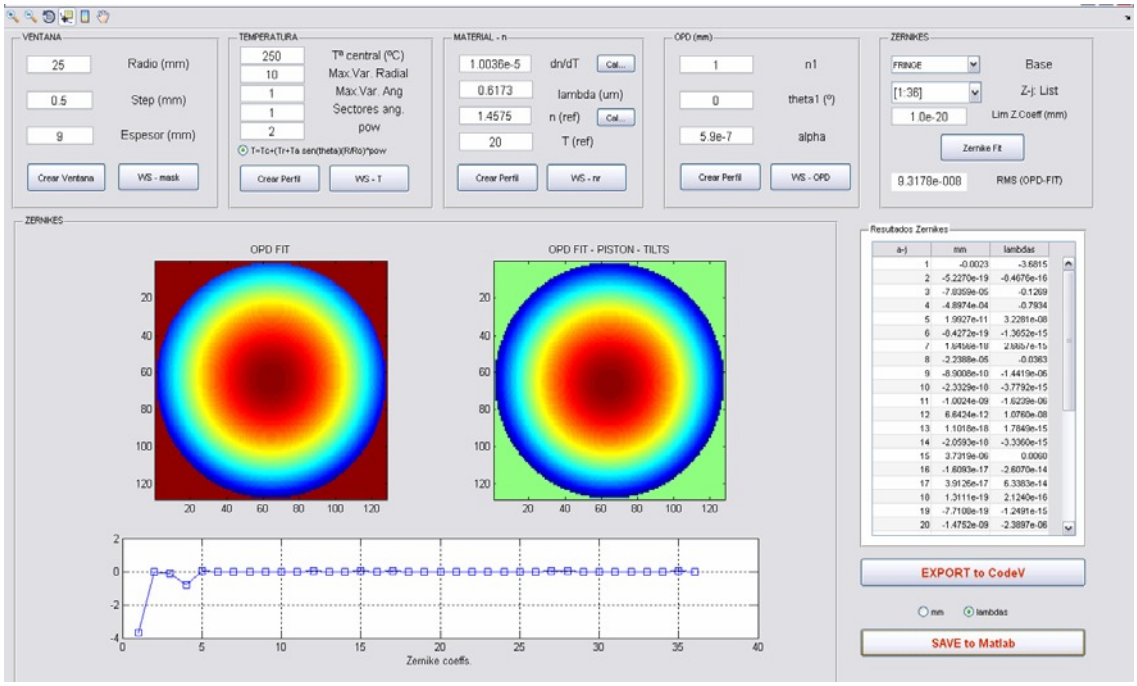

Fig. 7. Graphical User Interface

V. THERMAL GRADIENTS STUDIED

The temperature parameters used as input of the simulation subsystem have been taken from simulation of the thermal environment for FDT HREW and the boundary conditions of the FDT feedthrough have been had in mind. The most critical cases are in the phase of the orbit closest to the sun, and they have been resumed in table 1. Case Hot 1 represents a thermal simulation in which the thermal gradients present pure radial symmetry. The case under study Hot 5 is the expression of a situation in which the radial symmetry is broken and the gradients are a little decentred.

REQUIREMENT	CASE HOT-1 CENTRED	CASE HOT-5 1º OFF AXIS
Max T (Window 1, space side)	232.3	235.4
Max T (Window 2, instrument side)	228.3	231.0
T0 (Window 1, space side)	232.3	235.4
T0 (Window 2, instrument side)	228.3	231.0
$\|\delta\|$	4	4
$\|\rho_1\|$	4	4
$\|\rho_2\|$	2.7	3
$\|d\rho_1(\alpha)\|$ ***(Window 1, space side)***	0.4	0.71
$\|d\rho_2(\alpha)\|$ ***(Window 2, instrument side)***	0.1	0.31

Table 1 Temperature parameters

Where *T0* is the temperature at the centre of the window, δ is the temperature difference between windows, ρ_1 and ρ_2 are the maximum radial thermal gradients for each window (respectively) and $d\rho_1$ and $d\rho_2$ are the maximum azimuthal thermal variation for each window (respectively).

In the figures 7 and 8 are represented the OPD and Zernike surfaces of case HOT-1 and HOT-5 respectively. The OPD plots have been obtained according to the model described in the previous sections.

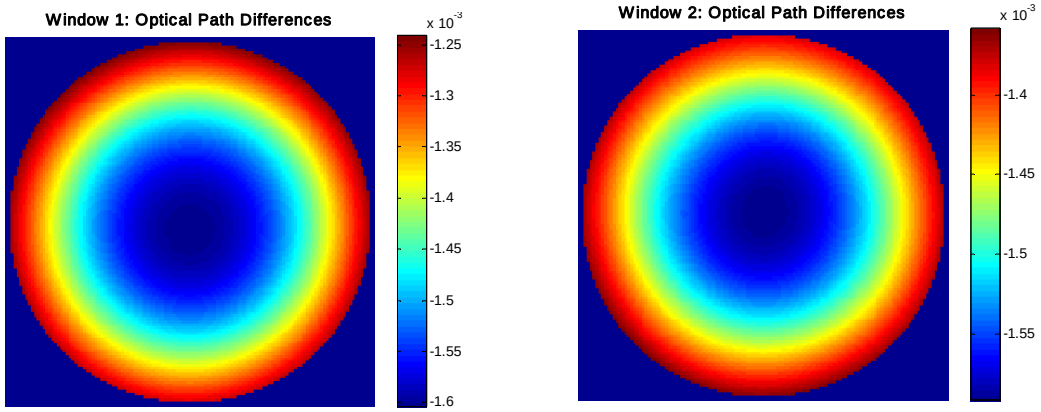

Fig. 8. OPD Case HOT-1 (Centred)

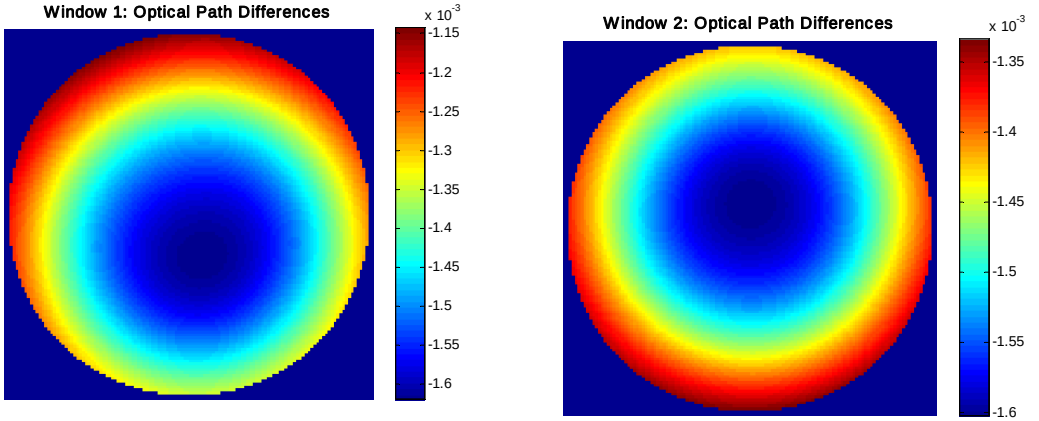

Fig. 9. OPD Case HOT-5 (1° Off axis)

The fig. 9 shows a little decentring of the gradient patter. The interpretation of such a decenter is understood as the tilt contribution due to the asymmetry of the observation mode. The boresight at focal plane location is also studied in the current simulation in order to assure the well location of the centre of the image at the focal plane position.

The HREW perturbed in vacuum condition for both cases HOT-1 and HOT-5 is added to the defocused FDT hot case. The optical parameters of the defocused system and after focusing are resumed in the following table.

	CASE HOT-1 ***CENTRED***	***CASE HOT-5*** ***1º OFF AXIS***
Distance between the HREW and the FDT*	322 mm	322 mm
FDT HREW perturbed + FDT hot case (defocused)	WFE = 0.226 λ	WFE = 0.226 λ
FDT HREW perturbed + FDT hot case (focused by L2 lens)	***WFE = 0.011*** λ	***WFE = 0.011*** λ
Displacement of L2 lens	***-0.30 mm***	***-0.30 mm***
Boresight at focal plane location HREW perturbed + FDT hot case (focused by L2 lens)	***x=-0.00074 y=-0.00125***	***x=-0.00076 y=-0.00125***

Table 2 HREW + FDT (Hot Case) Optical Parameters

An image simulation of the performance degradation at the image plane due to the temperature effect has been done taking an USAF test as object.

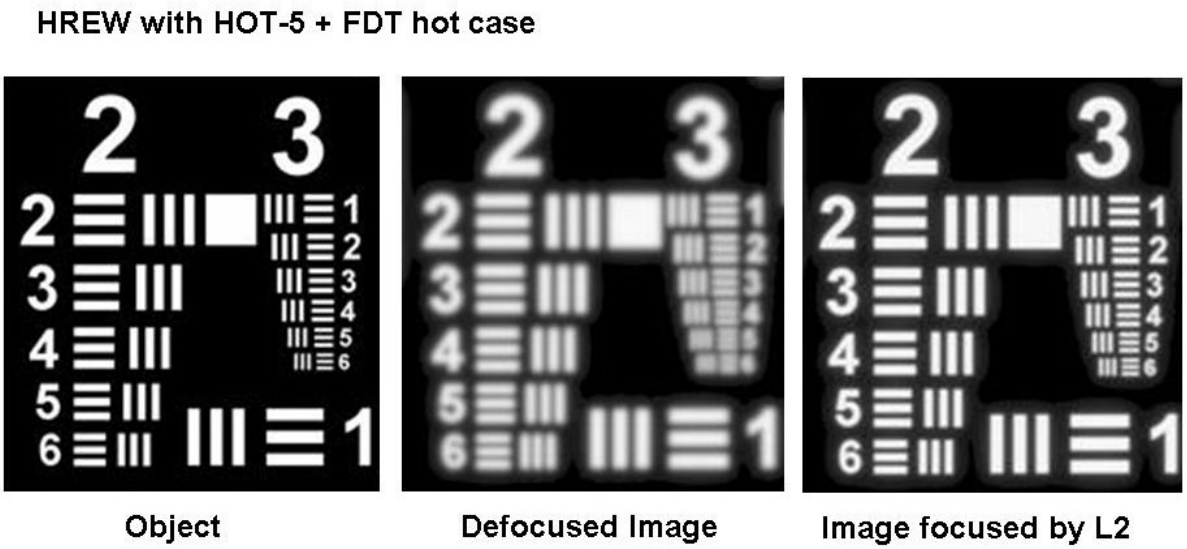

Fig. 10. Image simulation by CODE V

VI. CONCLUSIONS

The effects of FDT HREW thermal gradients on the FDT performance can be corrected by means of the PHI/FDT refocusing system and the image quality can be recovered at the scientific focal plane in both studied scenarios, the centred hot case (HOT-1) and the 1º off pointing hot case (HOT-5).

The boresight change due to the 1º off pointing thermal gradient is imperceptible at focal plane position.

Furthermore the authors wish to acknowledge with much appreciation the crucial help of the staff of "*Área de Instrumentación Óptica Espacial, Madrid, Spain*" to complete this study.

This study was supported by the Spanish MINECO (Ministerio de Economía y Competitividad) funded SO/PHI project ('AYA2012-39636-C06-01 Detailed design, manufacturing and integration of SO/PHI' and 'ESP2013-47349-C6-2R Manufacturing and integration of SO/PHI').

REFERENCES

[1] A. Gandorfer, S.K. Solanki, J. Woch, V. Martínez Pillet, A. Álvarez Herrero and T. Appourchaux, "The Solar Orbiter Mission and its Polarimetric and Helioseismic Imager (SO/PHI)", Journal of Physics: Conference Series 271 (2011), 012086.
[2] A. Álvarez-Herrero: "The polarization modulators based on liquid crystal variable retarders for the PHI and METIS instruments for the Solar Orbiter mission", proceeding 66598 at International Conference on Space Optics (ICSO 2014).
[3] V. Martínez-Pillet, J.C. del Toro-Iniesta, A. Alvarez-Herrero, et al., "The Imaging Magnetograph eXperiment (IMAX) for the Sunrise Balloon-Borne Solar Observatory," Solar Phys, 2011, 268, pp. 57-102.
[4] J. Barandiarán, "Solar Orbiter/ PHI Full Disk Telescope Entrance Window mechanical mount", proceeding 66273 at International Conference on Space Optics (ICSO 2014).
[5] M. Silva, J. A. Bonet-Navarro, A. Nuñez, A. Álvarez-Herrero, "Evaluation of the refocusing system of the Polarimetric Helioseismic Imager/Full Disk Telescope of the Solar Orbiter", proceeding 56569 at International Conference on Space Optics (ICSO 2014).
[6] Doyle, K., Genberg, V., Michels, G., Integrated Optomechanical Analysis, TT58 SPIE Press, 2002.
[7] Genberg, V. L., Michels, G. J., & Doyle, K. B. (2002, September). Making FEA results useful in optical analysis. In International Symposium on Optical Science and Technology (pp. 24-33). International Society for Optics and Photonics.
[8] Zemax data base
[9] Heckbert, Paul S., Pat Hanrahan, ''Beam Tracing Polygonal Objects'', Computer Graphics (SIGGRAPH'84 Proceedings), vol. 18, no. 3, July 1984, pp. 119-127.
[10] Heckbert, Paul S. "Writing a Ray Tracer." An Introduction to Ray Tracing.Andrew S. Glassner. London: Academic Press Limited, 1989. 263-294. Hardcover.